



Original article

Synthesis and evaluation of the apoptosis inducing and CT DNA interaction properties of a series of 4 β -carbamoyl 4'-O-demethylepipodophyllotoxins



Chun-Yan Sang^a, Jian-Fei Liu^a, Wen-Wen Qin^a, Jie Zhao^a, Lin Hui^{b,**}, Yong-Xin Jin^{d,**}, Shi-Wu Chen^{a,c,*}

^a School of Pharmacy, Lanzhou University, Lanzhou 730000, China

^b Experimental Center of Medicine, General Hospital of Lanzhou Military Command, Lanzhou 730050, China

^c Key Lab of Preclinical Study for New Drugs of Gansu Province, Lanzhou University, Lanzhou 730000, China

^d Department of Medicine, Second People's Hospital of Gansu Province, Lanzhou 730000, China

ARTICLE INFO

Article history:

Received 26 July 2013

Received in revised form

25 September 2013

Accepted 30 September 2013

Available online 6 October 2013

Keywords:

Podophyllotoxin

Carbamates

Cytotoxicity

Apoptosis

CT DNA

ABSTRACT

A series of carbamate derivatives of 4'-demethylepipodophyllotoxin have been synthesized, and their cytotoxicities against several human cancer cell lines, including HeLa, A549, HCT-8, and HL-60 cells, evaluated. Some of these compounds exhibited higher levels of cytotoxicity than the anticancer drug etoposide. 4 β -4'-Demethylepipodophyllotoxin 1-(4-nitrophenyl) piperazinyl carbamate (**19**) was found to be the most potent compound of those synthesized in the current study, and induced cell cycle arrest in the G2/M phase in HeLa cells, which was accompanied by apoptosis. Furthermore, this compound activated the expression of Bax, p53 and caspase-3 in HeLa cells, leading to changes in the conformation of calf thymus DNA from the B-form to a more compact C-form.

© 2013 Elsevier Masson SAS. All rights reserved.

1. Introduction

Current advances in cancer research consider the apoptosis, other than occurring in various physiological events, as crucially involved in the regulation of tumor growth as well as in the treatment response. Most of the anticancer strategies used in clinical oncology such as chemotherapy, γ -irradiation, including suicide gene therapy or immunotherapy, have been related to the activation of apoptosis signal transduction pathways in cancer cells [1]. Deeper investigations on molecular basis of apoptosis modulation open promising ways for a more rational approach to develop new therapeutic strategies [2]. Therefore, the design of new compounds able to modulate the apoptotic process, both as activators or inhibitors, represents an important strategic therapeutic approach in cancer disease [3].

Podophyllotoxin (PPT, **1**), extracted from the roots and rhizomes of *Podophyllum* species such as *Podophyllum hexandrum* and *Podophyllum peltatum* [4], has cathartic, antirheumatic and antiviral properties, and antimitotic activity [5]. By using PPT as a lead compound, structural modification of it leads to the emergence of less toxic, useful anti-cancer drugs namely, etoposide (VP-16, **2**) and teniposide (VM-26, **3**), which are thus successfully utilized in treatment of a variety of cancers, including small-cell lung cancer, testicular carcinoma, lymphoma, and Kaposi's sarcoma [6]. However, their therapeutic uses are often hindered by problems such as poor water-solubility and acquired drug-resistance [7]. To overcome these problems, extensive synthetic efforts have been carried out by a number of researchers, which leads to the development of several potential drug candidates based on PPT applied in clinical trial, such as, etopophos (**4**), NPF [8], GL-331 [9], tafluposide (F11782, **5**) [10] and F14512 (**6**) [11] (Fig. 1). Among them, etopophos, a water-soluble prodrug of **2**, was developed and approved for intravenous use in 1996. As a phosphate, **4** is readily converted in vivo by endogenous phosphatase to the active drug **2** and exhibits pharmacological and pharmacokinetic profiles similar to those of **2** [12].

* Corresponding author. School of Pharmacy, Lanzhou University, Lanzhou 730000, China. Tel./fax: +86 0931 8915686.

** Corresponding authors.

E-mail addresses: chenshw@lzu.edu.cn, chenshwu@gmail.com (S.-W. Chen).

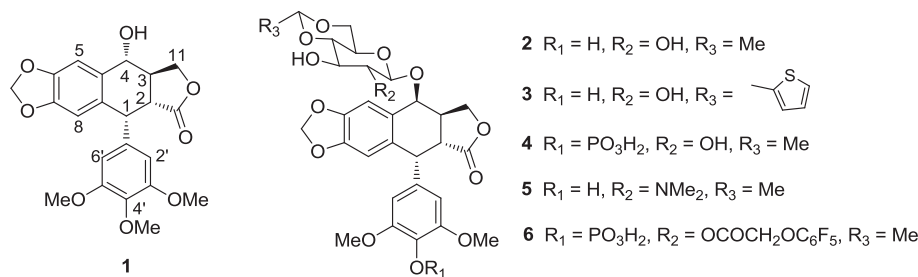


Fig. 1. Structures of podophyllotoxin (1), etoposide (2), teniposide (3), etopophos (4), NK-611 (5) and tafluposide (6).

Actually, since the discovery of PPT as an antimitotic antitumor agent, investigation of the structure–activity relationships of PPT indicates that the *trans*-lactone, the 4β -substituted moiety, and the $4'$ -demethyl moieties are essential for TOP-II inhibitory activity [13]. According to SAR of PPT, the replacement of the C-4 sugar moiety of etoposide with a nonsugar substitution has proven to be significant in overcoming the drug resistance of etoposide. The C-4 non-sugar substitutions can be linked through O-, S- or N-linkage [14], compare with the N-linked and S-linked compounds, the O-linked (ethers, esters) congeners show promising antitumor activity [15].

Recently, a series of 4β -carbamoyl epipodophyllotoxins have been generated, and shown to exhibit more potent anticancer activity and better binding ability to TOP-II than etoposide [16]. In this study, which is part of our continuing effort to find new podophyllotoxin-based compounds with potent activities [17–23], we synthesized a series of 4β -carbamoyl $4'$ -O-demethylepipodophyllotoxin and evaluated their cytotoxicities against a panel of four human cancer cell lines. Especially, the most active carbamate (19) was evaluated for its effect on apoptosis and interaction with Calf thymus DNA (CT DNA).

2. Results and discussion

2.1. Chemistry

Organic carbamates have frequently been employed as pharmaceuticals in the forms of drugs and prodrugs [24]. In recent years, several reports have indicated that the carbamate linkage present in the active pharmacophores of various structurally diverse molecules increases the biological activities of semi-synthetic/synthetic natural/synthetic molecules [25,26]. In this work, we synthesized 17 4β -carbamates of $4'$ -demethylepipodophyllotoxin (DMEP, 7) (11–27) by the route depicted in Scheme 1. PPT (1) was regioselectively demethylated with trimethylsilyl iodide (TMSI) and barium carbonate to afford 7 by means of a previously described procedure [27]. Then the $4'$ -hydroxyl of 7 was subsequently protected with chlorocarbonylbenzoate (Cbz-Cl) to give 8. Then the 4 -hydroxy of 8 was activated by treatment with *p*-nitrophenylchloroformate in pyridine to provide 9. Lastly, reaction of 9 with various amines in the presence of triethylamine and 4-dimethylaminopyridine (DMAP) afforded carbamates 11–25 in good to moderate yields. In addition, compounds 26 and 27 were also prepared by two steps to investigate the effects of free $4'$ -OH of PPT derivatives. Specially, the $4,4'$ -hydroxyl of 7 were activated simultaneously to afford 10, and reacting 10 with morphine or *p*-nitrobenzylpiperazine generated target compounds 26 and 27 as similar above procedure. All the synthesized compounds were characterized by IR, ^1H - and ^{13}C NMR spectroscopy, and high-resolution mass spectrometry. In the ^1H NMR spectra, the

formation of the carbamates of 7 was confirmed by the presence of a peak for the C-4 proton of DMEP at a chemical shift of ~ 6.05 ppm.

3. Biological results and discussion

3.1. Cytotoxicities of derivatives of 11–27

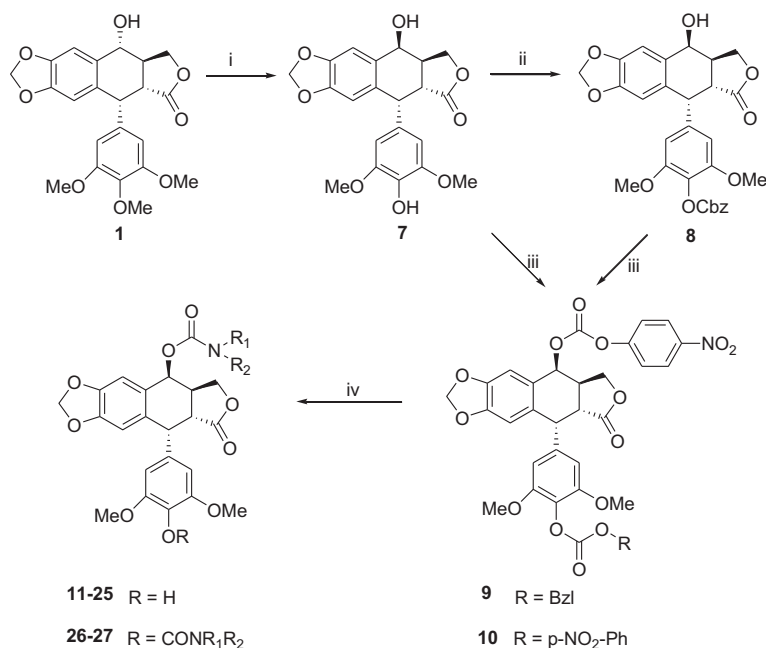
The *in vitro* cytotoxicities of carbamates 11–27 were evaluated against a panel of four human tumor cell lines (cervical carcinoma HeLa, lung carcinoma A-549, human colorectal adenocarcinoma HCT-8 and premyelocytic leukemia HL-60), with etoposide as a reference compound. The screening procedure was based on the standard MTT or CCK-8 method [21], and the results are summarized in Table 1.

All the carbamates showed substantial cytotoxicity and displayed IC_{50} values in the nanomolar range against the HL-60 and HCT-8 cell lines; that is, they were even more cytotoxic than etoposide. The IC_{50} value of compound 19, which is the most promising in this group compounds, is 0.074, 1.67, <0.01 and $0.17 \mu\text{M}$ for HeLa, A549, HCT-8 and HL-60, respectively. The other compounds generally showed moderate cytotoxicities against HeLa and A-549 cells lines.

Based on these results, we deduced some preliminary structure–activity relationships. First, the large activity range of compounds 11–19 indicated that the substituent of the amines markedly affected the activity profiles of this compound class, and the compounds with piperazines incorporated appear to be more potent than those with alkyl amines (11–14 vs 15–19). Second, the compounds with amino acids incorporated appear to be less potent than those with *p*-nitrobenzylpiperazine directly (20–25 vs 19), and the compounds with L-amino acids incorporated appear to be more potent than those with D-amino acid (22 vs 23, 24 vs 25). Lastly, compounds which contain only one substituent at the C-4 position showed superior activities in comparison with compounds simultaneously substituted at the C-4 and C-4' position of DMEP (15 vs 26, 19 vs 27). This observation is in accord with the previously reported SARs, the hydroxyl at C-4' position of PPT is necessary to remain their anticancer activity [28]. The data above revealed that 19 might serve as a potential anti-cancer drug, and we chose HeLa cells to further investigate the mechanism of its cytotoxic effect.

3.2. Cell cycle arrest and apoptosis induction

In our previous publication, we found some carbamate derivatives of 4β -(1,2,3-triazol-1-yl)podophyllotoxin induced cell cycle arrest in the G2/M phase accompanied by apoptosis in A-549 cells [22]. To determine whether 19 have similar effects on tumor cells, we investigated its effects on cell cycle progression by means of fluorescence-activated cell sorting analysis of HeLa cells stained with propidium iodide (Fig. 2) [22]. Treatment of the HeLa cells



Compd	NR ₁ R ₂	Compd	NR ₁ R ₂	Compd	NR ₁ R ₂
11		17		23	
12		18		24	
13		19		25	
14		20		26	
15		21		27	
16		22			

Scheme 1. Synthesis of compounds **11–27**. Reagents and conditions: i) TMSI then BaCO₃; ii) PhCH₂OCOCl, Et₃N, CH₂Cl₂; iii) p-NO₂PhOCOCl, pyridine; iv) HNR₂R₃, DMAP/Et₃N, CH₂Cl₂.

with **19** resulted in time- and dose-dependent accumulation of cells in the G₂/M phase with a concomitant decrease in the population of G₁ phase cells. G₂/M phase arrest was initially detectable after 12 h of treatment; 29.9% and 38.1% of the cells were in the G₂/M phase after exposure to **19** for 12 h and 24 h, respectively. In contrast, 22.7% of the cells were in this phase in untreated cultures (Fig. 2A). Furthermore, a population of sub-G₁ phase cells, which are characteristic apoptotic cells, was observed after 12 h of treatment with **19**. In control HeLa cells (Fig. 2A), only ~1.8% of the cells were in the sub-G₁ phase, whereas about 4.1% and 11.1% of cells were in the sub-G₁ phase after treatment with 5 μM **19** for 12 h and 24 h, respectively. Similar effects can be found in the dose-dependent manner (Fig. 2B). These results demonstrate that **19** interfered with cell proliferation by arresting the cell cycle and that

this compound induced G₂/M arrest accompanied by apoptosis in HeLa cells.

3.3. Effects of **19** on Bax, p53 and caspase-3 activation

Apoptosis or programmed cell death is a physiological process that provides an effective, non-inflammatory way to remove redundant or damaged cells from tissues thereby securing tissue homeostasis [29]. Inhibition of apoptosis is considered as an essential step in tumorigenesis and is one of the hallmarks of cancer, allowing the survival of cells that accumulate oncogenic events that otherwise would have been removed by apoptosis [30]. A multitude of signals activated by variable triggers, such as pro-apoptotic gene, tumor-suppressor gene and growth factors, cell–

Table 1
Cytotoxicities of compounds **11–27** (μM) at drugs exposure for 48 h.

Compounds	Cytotoxicity (IC_{50} , μM) ^a			
	HL-60 ^b	A-549 ^c	HeLa ^c	HCT-8 ^c
11	0.09	8.83	13.15	0.185
12	0.16	18.27	10.78	0.08
13	0.21	4.54	3.75	0.33
14	0.27	26.12	5.40	1.24
15	0.01	8.55	8.59	0.15
16	0.19	4.18	20.04	0.03
17	<0.01	3.89	4.40	1.62
18	0.33	5.24	1.58	0.01
19	0.17	1.67	0.074	<0.01
20	0.13	19.03	>100	0.71
21	0.26	8.32	>100	0.01
22	0.01	>100	49.43	0.57
23	0.02	>100	>100	0.85
24	0.03	9.55	4.13	0.01
25	0.04	>100	28.60	0.07
26	<0.01	>100	>100	0.13
27	0.35	56.9	>100	0.01
VP-16	1.15	3.20	2.91	7.06

^a Data are the mean of three independent experiments.

^b CCK-8 method.

^c MTT method.

cell interactions, changing nutrient conditions, hypoxic conditions, and cytotoxic damage affect the status of the apoptotic machinery [31]. To further explore the apoptotic pathway of **19** in cells, effects of **19** on Bax, p53 and caspase-3 activation in HeLa cells were performed by western blotting [32]. As shown in Figure 3, **19** significantly affected the expression of these three proteins, except for a marked increase of the pro-apoptotic protein Bax, tumor-suppressor gene p53, and caspase-3. We also observed a clear activation of Bax, p53 and caspase-3 in HeLa cells in a time-dependent manner, these results suggest that **19** induced apoptosis by means of multiple pathways.

3.4. Interaction of **19** with CT DNA

Ordinary, the analogs of **2** were considered as inhibitors of TOP-II, however, other compounds, which showed potent inhibitions against tumor cell lines, but not inhibitions to TOP-II were also found [33]. In order to study the interaction of **19** with CT DNA in pH 7.2 PBS, the CD spectrum of CT DNA and its complexes with **19** at various concentrations: 0 (1), 5 (2), 10 (3), 20 (4) and 40 (5) $\mu\text{g}/\text{mL}$ were recorded from 200 to 300 nm at 5 °C on a Jasco-810 spectrometer, and the CD spectra of CT DNA in the presence and absence of **19** in pH 7.2 PBS were showed in Figure 4A. The CD spectrum of free CT DNA exhibited a negative peak at 245 nm due to the helicity and a positive peak at 275 nm due to the base stacking (Fig. 4A, curve 1), which is the characteristic of DNA in the right hand B form [34,35]. Increasing the concentration of **19** ($c = 5, 10, 20, 40 \mu\text{g}/\text{mL}$, resp.) in above CT DNA solution, the intensity of positive band decreases and negative band increases, as well as a gradual blue shift of the negative band from 245 to 243 nm (Fig. 4, curve 1, 2, 3, 4, resp.), suggesting that DNA bound with **19** induces certain conformational changes, DNA double helix in solution is in a more helical state belonging to C form DNA [36–38].

A binding assay of with CT DNA was also performed by monitoring the changes in the emission spectral pattern of compound **19** (0.5 mM, excited at 383 nm) in the presence of increasing concentration of CT DNA (0, 1, 2, 3, 4, 5, 6 μM) in pH 7.2 PBS. Even though no appreciable change in the position of the charge transfer band of the complex was observed upon addition of DNA, the fluorescence intensity of the complex increases progressively with increasing

concentration of DNA (Fig. 4B), suggesting that compound **19**-based emission is enhanced when it is bound to DNA [39].

4. Conclusions

In summary, carbamate derivatives of 4 β -4'-demethylepipodophyllotoxin (**11–27**) showed promising *in vitro* cytotoxicities against a panel of human cancer cell lines. Fluorescence-activated cell sorting analysis indicated that **19** induced cell cycle arrest in the G2/M phase and apoptosis by activated Bax, p53 and caspase-3 in HeLa cells. In addition, **19** interacted with CT DNA in PBS, and caused the conformation of CT DNA changed from the B-form to a more compact C-form. These results suggest that these compounds have potential for further development as anticancer agents.

5. Experimental

5.1. Chemistry

Melting points were determined in Kofler apparatus and were uncorrected. IR spectra were measured on a Nicolet 5DX-FT-IR spectrometer on neat samples placed between KBr plates. ¹H NMR and ¹³C NMR spectra were recorded with a Varian Mercury-400BB and Mercury-600BB spectrometer with TMS as an internal standard, all chemical shift values are reported as δ ppm. Optical rotations were measured on a Perkin Elmer 341 polarimeter in a 1 dm cell at 23 °C. Mass spectra were recorded on a Bruker Daltonics APEXII49e and VGZAB-HS (70 eV) spectrometer with ESI source as ionization, respectively. All reactions were monitored by thin layer chromatography (TLC) on silica gel GF₂₅₄ (0.25 mm thick). Column chromatography (CC) was performed on Silica Gel 60 (230–400 mesh, Qingdao Ocean Chemical Ltd., China). Podophyllotoxin was isolated from a Chinese medicinal herb *Podophyllum emodi* Wall var Chinese Sprague, other starting materials and reagents were purchased commercially and used without further purified, unless otherwise stated.

5.1.1. General procedure of synthesis of **8**

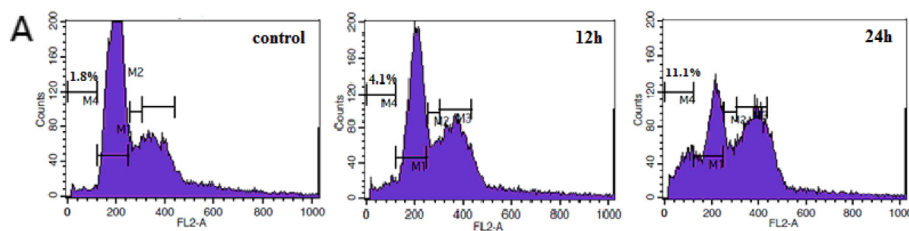
To **7** (384 mg, 0.96 mmol) in 6 ml acetone was added pyridine (0.36 ml, 4.4 mmol) and Cbz-Cl (0.4 ml, 2.8 mmol) at 0 °C. The reaction mixture was stirred at r.t. for 3 h, and then ice was added. The organic layer was washed with water, and dried over MgSO₄. The solvent was removed in vacuo and the crude product was purified by silica gel chromatography to give **8**.

5.1.2. General preparation of compounds **9/10**

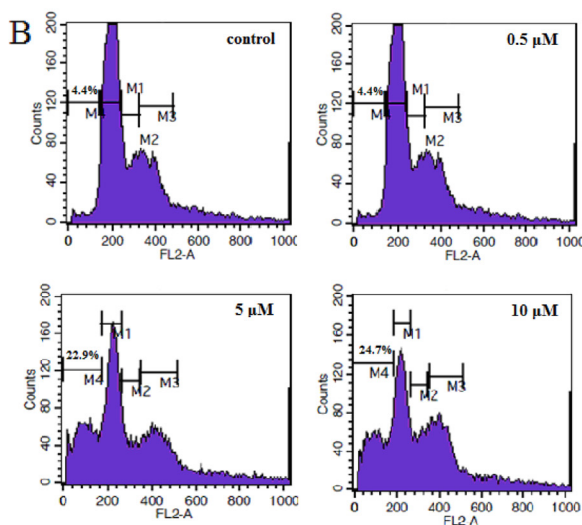
To a solution of *p*-nitrophenylchloroformate (36 mmol) in anhydrous CH₂Cl₂ (35 ml) was added dry pyridine (4.4 ml). Instantaneously a white precipitate was formed. A solution of **7** (or **8**) (12 mmol) in anhydrous CH₂Cl₂ (10 ml) was added dropwise under an argon atmosphere and allowed the mixture was stirred for further 45 min at room temperature. The mixture was purified by silica gel chromatography using a mixture of dichloromethane: ethyl acetate = 8:1 as the eluent to afford compounds **9** and **10**.

5.1.3. General preparation of compounds **11–27**

To a stirred solution of **9** (or **10**) (0.1 mmol) in dry dichloromethane (5 ml) was added the appropriate amine (0.15 mmol, 1.5 equiv), triethylamine (0.11 mmol) and DMAP (0.11 mmol) at room temperature. After stirring for overnight, the reaction mixture was washed with cold saturated NaHCO₃ and then water until pH 6–7. The extract was dried over MgSO₄ and concentrated in vacuo at 30 °C. The residue was purified by silica gel column chromatography using a mixture of petro ether/ethyl acetate 1:1 as the eluent to afford compounds **11–27** in the reported yields.



Compounds	Sub-G1 (M4)	G1 (M1)	S (M2)	G2/M (M3)
Control	1.8%	57.2%	9.0%	22.7%
12 h	4.1%	43.8%	10.2%	29.9%
24 h	11.1%	33.3%	10.2%	38.1%



	control	0.5 μM	5 μM	10 μM
Sub-G1 (M4)	4.4	21.7	23.0	24.7
G1 (M1)	54.7	35.9	33.9	26.0
S (M2)	16.3	9.8	10.2	13.1
G2/M (M3)	15.0	20.5	22.5	29.1

Fig. 2. Effect of **19** on cell cycle progression.

5.1.3.1. 4'-Demethylepipodophyllotoxin 4β-[N-(n-propyl)] carbamate (**11**). Yield: 56%; white powder solid; mp: 184–186 °C; $[\alpha]_D^{23} -29^\circ$ (c 0.1, CHCl₃); IR (KBr cm⁻¹) 3417, 2963, 1776, 1714, 1613, 1515, 1482, 1460, 1332, 1233, 1115, 1038, 999; ¹H NMR (400 MHz, CDCl₃) δ 6.93 (s, 1H), 6.54 (s, 1H), 6.29 (s, 2H), 6.01 (t, J = 4.4 Hz, 2H), 5.97 (s, 1H), 4.78 (t, J = 5.6 Hz, 1H), 4.64 (d, J = 4.8 Hz, 1H), 4.37 (t, J = 4.4 Hz, 1H), 3.99 (t, J = 5.2 Hz, 1H), 3.77 (s, 6H), 3.20–3.15 (m, 2H), 3.00–2.91 (m, 1H), 1.59–1.50 (m, 2H), 0.94 (t, J = 14.4 Hz, 3H); ¹³C NMR (100 MHz, CDCl₃) δ 174.7, 156.0, 148.9, 147.5, 146.6, 134.2, 133.0, 130.2, 128.3, 110.2, 109.7, 107.8 (2C), 101.7, 68.6, 67.8, 58.6, 56.5 (2C), 43.8, 43.0, 41.7, 37.2, 23.2, 18.5, 11.3; HRMS (ESI) 508.1571 for [M + Na]⁺ (calcd 508.1578 for C₂₅H₂₇NNaO₉).

5.1.3.2. 4'-Demethylepipodophyllotoxin 4β-(N-cyclopropyl) carbamate (**12**). Yield: 71%; white powder solid; mp: 182–184 °C; $[\alpha]_D^{23} -32^\circ$ (c 0.1, CHCl₃); IR (KBr cm⁻¹) 3434, 2955, 2905, 1768, 1712, 1612, 1519, 1482, 1460, 1309, 1222, 1185, 1112, 1030, 992; ¹H NMR (600 MHz, CDCl₃) δ 6.94 (s, 1H), 6.54 (s, 1H), 6.28 (s, 2H), 6.00 (t, J = 4.8 Hz, 2H), 5.97 (s, 1H), 5.44 (s, 1H), 4.99 (s, 1H), 4.63 (d, J = 4.2 Hz, 1H), 4.38 (t, J = 8.4 Hz, 1H), 3.98 (t, J = 3.0 Hz, 1H), 3.78 (s, 6H), 3.14 (d, J = 3.6 Hz, 1H), 2.96 (d, J = 4.8 Hz, 1H), 1.62 (s, 1H), 0.78 (d, J = 5.4 Hz, 2H), 0.55 (d, J = 6.0 Hz, 2H); ¹³C NMR (150 MHz, CDCl₃) δ 174.5, 156.5, 148.9, 147.4, 146.5, 134.1, 132.9, 130.1, 128.1, 110.1, 109.7, 107.7 (2C), 101.6, 68.6, 67.6, 56.4 (2C), 53.8, 43.6, 41.6, 37.0, 31.7, 6.9 (2C); HRMS (ESI) 506.1413 for [M + Na]⁺ (calcd 506.1422 for C₂₅H₂₅NNaO₉).

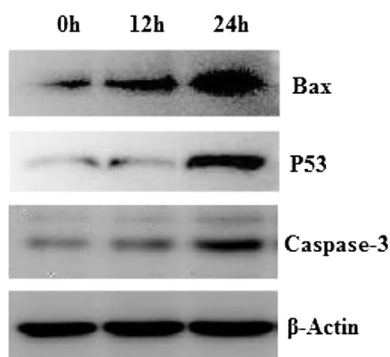


Fig. 3. Effects of compound **19** on cellular levels of Bax, p53 and caspase-3. HeLa cells were incubated with 5 μ M **19** for 0 h, 12 h, 24 h, and cell lysates were prepared and analyzed by Western blotting.

5.1.3.3. 4'-Demethylepipodophyllotoxin 4 β -(*N*-cyclopentyl) carbamate (13**).** Yield: 60%; white powder solid; mp: 241–243 °C; $[\alpha]_D^{23} -28^\circ$ (c 0.1, CHCl₃); IR (KBr cm⁻¹) 3421, 2957, 1776, 1710, 1613, 1514, 1483, 1459, 1331, 1232, 1115, 1037, 998; ¹H NMR (400 MHz, CDCl₃) δ 6.93 (s, 1H), 6.54 (s, 1H), 6.29 (s, 2H), 6.00 (t, *J* = 4.8 Hz, 2H), 5.97 (s, 1H), 4.64 (d, *J* = 4.8 Hz, 1H), 4.38 (t, *J* = 5.2 Hz, 1H), 4.02–3.96 (m, 1H), 3.77 (s, 6H), 3.17 (dd, *J* = 9.2, 4.4 Hz, 1H), 3.00–2.88 (m, 1H), 2.00–1.95 (m, 2H), 1.69–1.60 (m, 5H), 1.42–1.36 (m, 2H); ¹³C NMR (100 MHz, CDCl₃) δ 174.7, 155.4, 149.0, 146.7 (2C), 134.3, 133.0, 130.2, 118.4, 110.3, 109.7, 107.9 (2C), 101.7, 68.5, 67.8, 56.5 (2C), 53.1, 43.8, 41.8, 37.3, 33.4, 33.3, 23.7 (2C); HRMS (ESI) 529.2189 for [M + NH₄]⁺ (calcd 529.2181 for C₂₇H₃₃N₂O₉).

5.1.3.4. 4'-Demethylepipodophyllotoxin 4 β -(*N*-cyclohexyl) carbamate (14**).** Yield: 71%; white powder solid; mp: 262–264 °C; $[\alpha]_D^{23} -29^\circ$ (c 0.1, CHCl₃); IR (KBr cm⁻¹) 3432, 2931, 1776, 1711, 1617, 1513, 1484, 1457, 1230, 1117, 1036, 1001; ¹H NMR (400 MHz, CDCl₃) δ 6.92 (s, 1H), 6.54 (s, 1H), 6.29 (s, 2H), 6.00 (t, *J* = 5.6 Hz, 2H), 5.97 (s, 1H), 4.64 (t, *J* = 7.2 Hz, 1H), 4.37 (t, *J* = 5.6 Hz, 1H), 3.98 (t, *J* = 5.2 Hz, 1H), 3.78 (s, 6H), 3.17 (dd, *J* = 8.0, 4.8 Hz, 1H), 3.14–2.92 (m, 1H), 1.96 (d, *J* = 11.2 Hz, 2H), 1.72 (t, *J* = 13.6 Hz, 2H), 1.63–1.60 (m, 2H), 1.31 (s, 1H), 1.28–1.08 (m, 2H); ¹³C NMR (100 MHz, CDCl₃) δ 174.7, 155.1, 148.9, 147.5, 146.7 (2C), 134.3, 133.0, 130.2, 128.4, 110.3, 109.7, 107.9 (2C), 101.7, 68.5, 67.9, 56.6 (2C), 50.3, 43.8, 41.8, 37.3, 33.4, 25.5, 24.8, 18.5 (2C); HRMS (ESI) 543.2334 for [M + NH₄]⁺ (calcd 543.2337 for C₂₈H₃₅N₂O₉).

5.1.3.5. 4'-Demethylepipodophyllotoxin 4 β -(*N*-morpholino) carbamate (15**).** Yield: 67%; white powder solid; mp: 208–210 °C;

$[\alpha]_D^{23} -52^\circ$ (c 0.1, CHCl₃); IR (KBr cm⁻¹) 3389, 2900, 1770, 1692, 1612, 1520, 1505, 1480, 1462, 1245, 1222, 1113, 1027, 993; ¹H NMR (400 MHz, CDCl₃) δ 6.93 (s, 1H), 6.55 (s, 1H), 6.29 (s, 2H), 6.07 (d, *J* = 3.2 Hz, 1H), 6.00 (dd, *J* = 7.6, 4.8 Hz, 2H), 4.65 (t, *J* = 4.8 Hz, 1H), 4.38 (t, *J* = 5.6 Hz, 1H), 4.00–3.92 (m, 1H), 3.78 (s, 6H), 3.70 (s, 2H), 3.68 (s, 2H), 3.50 (s, 2H), 3.42 (s, 2H), 3.14 (dd, *J* = 7.2, 4.8 Hz, 1H), 3.02–2.93 (m, 1H); ¹³C NMR (100 MHz, CDCl₃) δ 174.6, 154.9, 149.0, 147.5, 146.7, 134.4, 133.0, 130.0, 128.2, 110.2, 109.7, 107.9 (2C), 101.7, 69.6, 67.8, 66.7, 58.5 (2C), 56.6 (2C), 43.7, 41.9, 37.2, 18.5 (2C); HRMS (ESI) 531.1985 for [M + NH₄]⁺ (calcd 531.1973 for C₂₆H₃₁N₂O₁₀).

5.1.3.6. 4'-Demethylepipodophyllotoxin 4 β -[*N*-(*N*-methyl piperazinyl)] carbamate (16**).** Yield: 57%; white powder solid; mp: 210–213 °C; $[\alpha]_D^{23} -56^\circ$ (c 0.1, CHCl₃); IR (KBr cm⁻¹) 3415, 2928, 1771, 1694, 1612, 1519, 1481, 1460, 1426, 1233, 1111, 1048, 996; ¹H NMR (400 MHz, CDCl₃) δ 6.93 (s, 1H), 6.54 (s, 1H), 6.29 (s, 2H), 6.05 (d, *J* = 3.6 Hz, 2H), 6.00 (d, *J* = 3.6 Hz, 1H), 4.65 (d, *J* = 4.8 Hz, 1H), 4.38 (t, *J* = 4.4 Hz, 1H), 3.97–3.92 (m, 1H), 3.78 (s, 6H), 3.60–3.42 (m, 4H), 3.15 (dd, *J* = 7.2, 4.8 Hz, 1H), 2.99–2.92 (m, 1H), 2.43–2.30 (m, 7H); ¹³C NMR (100 MHz, CDCl₃) δ 174.6, 154.8, 148.9, 147.5, 146.7 (2C), 134.3, 133.0, 130.1, 128.4, 110.2, 109.8, 107.8 (2C), 101.7, 69.3, 67.9, 58.6, 56.6 (2C), 54.8, 46.3, 44.0, 43.0, 41.9, 37.2, 18.6; HRMS (ESI) 527.2021 for [M + H]⁺ (calcd 527.2024 for C₂₇H₃₁N₂O₉).

5.1.3.7. 4'-Demethylepipodophyllotoxin 4 β -[*N*-[1-(4-cyclopentyl piperazinyl)]] carbamate (17**).** Yield: 59%; white powder solid; mp: 140–142 °C; $[\alpha]_D^{23} -33^\circ$ (c 0.1, CHCl₃); IR (KBr cm⁻¹) 3436, 2956, 1776, 1695, 1611, 1509, 1483, 1460, 1427, 1288, 1241, 1122, 1039, 1000; ¹H NMR (400 MHz, CDCl₃) δ 6.94 (s, 1H), 6.54 (s, 1H), 6.29 (s, 2H), 6.05 (d, *J* = 3.6 Hz, 1H), 5.99 (t, *J* = 7.2 Hz, 2H), 4.66 (d, *J* = 4.8 Hz, 1H), 4.39 (t, *J* = 6.4 Hz, 1H), 3.99–3.94 (m, 1H), 3.78 (s, 6H), 3.69 (s, 1H), 3.65–3.47 (m, 4H), 3.17 (dd, *J* = 7.2, 4.8 Hz, 1H), 2.98–2.95 (m, 1H), 2.55–2.44 (m, 4H), 2.38 (s, 1H), 1.84 (s, 2H), 1.71 (s, 2H), 1.69–1.66 (m, 2H), 1.57–1.36 (m, 2H); ¹³C NMR (100 MHz, CDCl₃) δ 174.6, 156.2, 154.8, 148.9, 147.5, 146.7 (2C), 134.3, 133.0, 130.2, 128.5, 112.0, 111.8, 107.9 (2C), 101.7, 69.2, 68.7, 67.4, 58.5 (2C), 56.6 (2C), 44.1, 41.9, 40.0, 30.4 24.2 (2C), 18.5 (2C); HRMS (ESI) 581.2485 for [M + H]⁺ (calcd 581.2494 for C₃₁H₃₇N₂O₉).

5.1.3.8. 4'-Demethylepipodophyllotoxin 4 β -[*N*-[1-(4-fluorophenyl piperazinyl)]] carbamate (18**).** Yield: 65%; white powder solid; mp: 152–153 °C; $[\alpha]_D^{23} -35^\circ$ (c 0.1, CHCl₃); IR (KBr cm⁻¹) 3436, 2916, 1778, 1696, 1613, 1510, 1483, 1460, 1428, 1231, 1116, 1039, 999; ¹H NMR (400 MHz, CDCl₃) δ 6.96 (t, *J* = 4.4 Hz, 2H), 6.95 (s, 1H), 6.89–6.86 (m, 2H), 6.56 (s, 1H), 6.30 (s, 2H), 6.08 (d, *J* = 3.6 Hz, 1H), 6.00–5.98 (m, 2H), 4.66 (d, *J* = 4.8 Hz, 1H), 4.39 (t, *J* = 6.4 Hz, 1H), 3.99–3.94 (m, 1H), 3.78 (s, 6H), 3.74 (d, *J* = 8.0 Hz, 2H), 3.59 (d, *J* = 6.8 Hz,

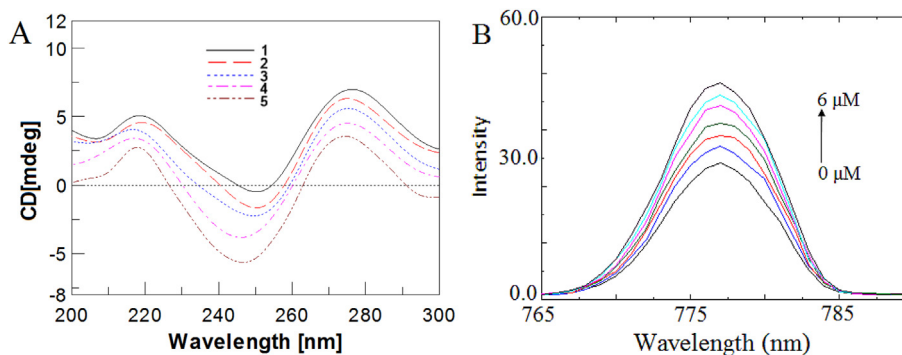


Fig. 4. Effects of **19** with CT-DNA. (A) Circular dichroism spectra of CT-DNA in the presence of increasing concentration of compound **19** in 10 mM PBS. 1. 25 μ g/mL CT-DNA, 2. 1 + 5 μ g/mL **19**, 3. 1 + 10 μ g/mL **19**, 4. 1 + 20 μ g/mL **19**, 5. 1 + 40 μ g/mL **19**. (B) Fluorescence spectra of compound **19** in the presence of increasing concentration of CT DNA. [compound **19**] = 1 μ M, [DNA] = 0, 1, 2, 3, 4, 5 and 6 μ M.

2H), 3.17 (dd, $J = 7.2, 4.8$ Hz, 1H), 3.09 (s, 2H), 3.03–2.97 (m, 3H); ^{13}C NMR (100 MHz, CDCl_3) δ 174.5, 156.2, 154.8, 149.0, 147.8, 147.6, 146.7 (2C), 134.3, 133.1, 130.1, 128.3, 119.0, 118.9, 116.0, 115.8, 110.2, 109.8, 108.0 (2C), 101.8, 69.5, 67.9, 56.6 (2C), 50.7 (2C), 44.2, 43.8 (2C), 40.0, 37.2; HRMS (ESI) 607.2089 for $[\text{M} + \text{H}]^+$ (calcd 607.2086 for $\text{C}_{32}\text{H}_{32}\text{FN}_2\text{O}_9$).

5.1.3.9. *4'-Demethylepipodophyllotoxin 4 β -[N-[1-(4-nitrophenyl)piperazinyl]] carbamate (19)*. Yield: 69%; yellow powder solid; mp: 154–156 °C; $[\alpha]_{\text{D}}^{23} -53^\circ$ (c 0.1, CHCl_3); IR (KBr cm^{-1}) 3464, 2908, 1777, 1697, 1596, 1506, 1484, 1428, 1324, 1232, 1114, 1039, 999; ^1H NMR (600 MHz, CDCl_3) δ 8.16–8.13 (m, 2H), 6.94 (s, 1H), 6.84–6.81 (m, 2H), 6.57 (s, 1H), 6.29 (s, 2H), 6.09 (d, $J = 3.6$ Hz, 1H), 5.99 (t, $J = 3.0$ Hz, 2H), 5.46 (s, 1H), 4.67 (d, $J = 5.4$ Hz, 1H), 4.39 (q, $J = 6.0$ Hz, 1H), 3.96 (q, $J = 6.6$ Hz, 1H), 3.76 (s, 6H), 3.68 (s, 2H), 3.61 (s, 2H), 3.48 (s, 2H), 3.39 (s, 2H), 3.17 (dd, $J = 7.2, 4.8$ Hz, 1H), 3.15–2.99 (m, 1H); ^{13}C NMR (150 MHz, CDCl_3) δ 174.3, 154.6, 154.3, 148.9, 147.4, 146.5, 139.1, 134.2, 132.9, 129.9, 127.9, 125.9 (2C), 113.1 (2C), 110.1, 109.5, 107.7, 101.6, 69.7, 69.5, 67.6, 56.4 (2C), 53.7, 46.7, 43.6, 43.1, 41.7, 37.0, 31.7, 29.2; HRMS (ESI) 656.1852 for $[\text{M} + \text{Na}]^+$ (calcd 656.1851 for $\text{C}_{32}\text{H}_{31}\text{N}_3\text{NaO}_{11}$).

5.1.3.10. *N-[1-oxyl-(4'-demethylepipodophyllotoxin)]-L-alanine-4-(4-p-nitrophenyl-piperazine) carbamate (20)*. Yield: 63%; yellow powder solid; mp: 177–179 °C; $[\alpha]_{\text{D}}^{23} -42^\circ$ (c 0.1, CHCl_3); IR (KBr cm^{-1}) 3429, 2914, 1777, 1716, 1646, 1596, 1507, 1484, 1456, 1326, 1230, 1113, 1018, 996; ^1H NMR (600 MHz, CDCl_3) δ 8.16 (d, $J = 9.0$ Hz, 2H), 6.92 (s, 1H), 6.85 (d, $J = 9.0$ Hz, 2H), 6.55 (s, 1H), 6.28 (s, 2H), 6.00 (t, $J = 7.2$ Hz, 2H), 5.98 (t, $J = 1.2$ Hz, 1H), 5.81 (d, $J = 6.0$ Hz, 1H), 5.45 (s, 1H), 4.68 (t, $J = 7.2$ Hz, 1H), 4.65 (d, $J = 4.8$ Hz, 1H), 4.32 (t, $J = 8.4$ Hz, 1H), 4.00 (q, $J = 4.8$ Hz, 1H), 3.90–3.87 (m, 1H), 3.77 (s, 8H), 3.67 (t, $J = 4.8$ Hz, 1H), 3.52–3.44 (m, 4H), 3.18 (dd, $J = 7.2, 4.8$ Hz, 1H), 2.98–2.92 (m, 1H), 1.63 (s, 1H), 1.40 (d, $J = 7.2$ Hz, 3H); ^{13}C NMR (150 MHz, CDCl_3) δ 174.3, 170.7, 155.1, 154.2, 148.9, 147.4, 146.5 (2C), 139.4, 134.1, 133.0, 127.9, 125.9 (2C), 113.3 (2C), 110.2, 109.5, 107.8 (2C), 101.6, 69.0, 67.4, 56.4 (2C), 47.1, 47.0, 46.9, 44.7, 43.6, 41.5 (2C), 37.0, 19.1; HRMS (ESI) 727.2225 for $[\text{M} + \text{Na}]^+$ (calcd 727.2222 for $\text{C}_{35}\text{H}_{36}\text{N}_4\text{NaO}_{12}$).

5.1.3.11. *N-[1-Oxyl-(4'-demethylepipodophyllotoxin)]-L-lysine-4-(4-p-nitrophenyl-piperazine) carbamate (21)*. Yield: 68%; yellow powder solid; mp: 170–171 °C; $[\alpha]_{\text{D}}^{23} -45^\circ$ (c 0.1, CHCl_3); IR (KBr cm^{-1}) 3429, 2911, 1776, 1713, 1642, 1596, 1507, 1484, 1459, 1326, 1229, 1114, 1093, 998; ^1H NMR (600 MHz, CDCl_3) δ 8.16 (d, $J = 7.2$ Hz, 2H), 6.90 (s, 1H), 6.85 (d, $J = 9.0$ Hz, 2H), 6.56 (s, 1H), 6.29 (s, 2H), 6.01 (s, 1H), 5.98 (d, $J = 6.0$ Hz, 2H), 5.60 (d, $J = 9.6$ Hz, 1H), 5.45 (s, 1H), 4.66 (d, $J = 6.4$ Hz, 1H), 4.55 (q, $J = 8.4$ Hz, 1H), 4.29 (t, $J = 8.4$ Hz, 1H), 3.97 (q, $J = 4.8$ Hz, 1H), 3.85 (t, $J = 8.4$ Hz, 2H), 3.77 (s, 8H), 3.49 (d, $J = 8.4$ Hz, 2H), 3.18 (dd, $J = 8.4, 4.8$ Hz, 1H), 2.97–2.92 (m, 1H), 2.00 (q, $J = 8.4$ Hz, 1H), 1.04 (d, $J = 6.6$ Hz, 3H), 0.91 (d, $J = 7.2$ Hz, 3H); ^{13}C NMR (150 MHz, CDCl_3) δ 174.2, 170.1, 156.0, 154.3, 148.9, 147.4, 146.5 (2C), 139.4, 134.1, 133.0, 127.9, 125.9 (2C), 113.2 (2C), 110.2, 109.3, 107.8 (2C), 101.6, 69.1, 67.4, 56.4 (2C), 55.7, 47.2, 46.9, 45.0, 41.5, 37.0, 29.7, 19.7, 17.1; HRMS (ESI) 755.2534 for $[\text{M} + \text{Na}]^+$ (calcd 755.2535 for $\text{C}_{37}\text{H}_{40}\text{N}_4\text{NaO}_{12}$).

5.1.3.12. *N-[1-Oxyl-(4'-demethylepipodophyllotoxin)]-L-methine-4-(4-p-nitrophenyl-piperazine) carbamate (22)*. Yield: 56%; yellow powder solid; mp: 199–201 °C; $[\alpha]_{\text{D}}^{23} -41^\circ$ (c 0.1, CHCl_3); IR (KBr cm^{-1}) 3436, 2919, 1776, 1713, 1638, 1598, 1507, 1484, 1325, 1233, 1115, 1035, 999; ^1H NMR (600 MHz, CDCl_3) δ 8.15 (d, $J = 12.0$ Hz, 2H), 6.91 (s, 1H), 6.85 (d, $J = 12.0$ Hz, 2H), 6.56 (s, 1H), 6.28 (s, 2H), 5.99 (q, $J = 6.0$ Hz, 3H), 5.70 (d, $J = 6.0$ Hz, 1H), 5.46 (s, 1H), 4.90 (q, $J = 6.0$ Hz, 1H), 4.65 (d, $J = 6.0$ Hz, 1H), 4.30 (t, $J = 9.0$ Hz, 1H), 3.96 (s, 1H), 3.85 (d, $J = 12.0$ Hz, 2H), 3.74 (s, 8H), 3.62 (s, 2H), 3.46 (t,

$J = 6.0$ Hz, 2H), 3.17 (d, $J = 12.0$ Hz, 1H), 2.94 (t, $J = 9.0$ Hz, 1H), 2.60–2.52 (m, 2H), 2.14 (s, 3H), 1.98 (s, 1H), 1.87 (s, 1H), 1.64 (s, 2H); ^{13}C NMR (150 MHz, CDCl_3) δ 174.2, 170.0, 155.7, 154.2, 148.9, 147.4, 146.4 (2C), 139.4, 134.1, 133.1, 130.0, 127.8, 125.9 (2C), 113.2 (2C), 110.2, 109.4, 107.8 (2C), 101.6, 69.2, 67.4, 56.4 (2C), 49.8, 47.2, 46.8, 44.8, 43.6, 41.6, 41.5, 37.0, 32.9, 30.2, 15.8; HRMS (ESI) 787.2256 for $[\text{M} + \text{Na}]^+$ (calcd 787.2256 for $\text{C}_{37}\text{H}_{40}\text{N}_4\text{NaO}_{12}\text{S}$).

5.1.3.13. *N-[1-Oxyl-(4'-demethylepipodophyllotoxin)]-D-methine-4-(4-p-nitrophenyl-piperazine) carbamate (23)*. Yield: 65%; yellow powder solid; mp: 172–175 °C; $[\alpha]_{\text{D}}^{23} -50^\circ$ (c 0.1, CHCl_3); IR (KBr cm^{-1}) 3411, 2918, 1776, 1713, 1645, 1596, 1507, 1484, 1454, 1325, 1232, 1114, 1034, 998; ^1H NMR (600 MHz, CDCl_3) δ 8.17 (d, $J = 9.0$ Hz, 2H), 6.89 (s, 1H), 6.86 (d, $J = 9.6$ Hz, 2H), 6.54 (s, 1H), 6.28 (s, 2H), 5.98 (d, $J = 12.6$ Hz, 2H), 5.70 (d, $J = 8.4$ Hz, 1H), 5.43 (s, 1H), 4.95–4.91 (m, 1H), 4.40 (d, $J = 6.0$ Hz, 1H), 4.38 (t, $J = 9.0$ Hz, 1H), 4.02 (q, $J = 8.4$ Hz, 1H), 3.89 (d, $J = 9.0$ Hz, 2H), 3.77 (s, 8H), 3.53–3.44 (m, 4H), 3.21 (dd, $J = 7.2, 4.8$ Hz, 1H), 3.00–2.94 (m, 1H), 2.62–2.54 (m, 2H), 2.14 (s, 3H), 2.02–1.97 (m, 1H), 1.93–1.97 (m, 1H), 1.58 (s, 3H), 1.26 (s, 1H); ^{13}C NMR (150 MHz, CDCl_3) δ 174.3, 169.9, 155.7, 154.3, 148.9, 147.3, 146.5 (2C), 139.5, 134.2, 133.0, 127.8, 125.9 (2C), 113.3 (2C), 110.2, 109.7, 107.8 (2C), 101.6, 69.2, 67.4, 56.5 (2C), 49.6, 47.3, 46.9, 44.8, 43.6, 41.6, 41.5, 37.0, 33.1, 30.3, 29.7, 15.9; HRMS (ESI) 787.2260 for $[\text{M} + \text{Na}]^+$ (calcd 787.2256 for $\text{C}_{37}\text{H}_{40}\text{N}_4\text{NaO}_{12}\text{S}$).

5.1.3.14. *N-[1-Oxyl-(4'-demethylepipodophyllotoxin)]-L-phenylalanine-4-(4-p-nitrophenyl-piperazine) carbamate (24)*. Yield: 72%; yellow powder solid; mp: 169–171 °C; $[\alpha]_{\text{D}}^{23} -31^\circ$ (c 0.1, CHCl_3); IR (KBr cm^{-1}) 3428, 2908, 2360, 1776, 1713, 1643, 1596, 1506, 1484, 1454, 1325, 1231, 1114, 1037, 997; ^1H NMR (600 MHz, CDCl_3) δ 8.13 (d, $J = 6.0$ Hz, 2H), 7.31 (t, $J = 6.0$ Hz, 2H), 7.23 (q, $J = 9.0$ Hz, 3H), 6.85 (s, 1H), 6.73 (d, $J = 6.0$ Hz, 2H), 6.55 (s, 1H), 6.29 (s, 2H), 6.01 (d, $J = 6.0$ Hz, 1H), 5.96 (d, $J = 6.0$ Hz, 1H), 5.71 (d, $J = 6.0$ Hz, 1H), 5.44 (s, 1H), 4.88 (t, $J = 9.0$ Hz, 1H), 4.65 (d, $J = 6.0$ Hz, 1H), 4.30 (t, $J = 9.0$ Hz, 1H), 3.97 (t, $J = 9.0$ Hz, 1H), 3.77 (s, 8H), 3.70 (d, $J = 6.0$ Hz, 1H), 3.50 (s, 1H), 3.22 (s, 2H), 3.09 (s, 2H), 2.99 (s, 1H), 2.93 (s, 1H), 2.73 (t, $J = 6.0$ Hz, 1H); ^{13}C NMR (150 MHz, CDCl_3) δ 174.2, 169.8, 155.1, 154.1, 148.9, 147.4 (2C), 146.5 (2C), 139.3, 135.7, 134.2, 133.0, 129.6 (2C), 128.8 (2C), 127.8, 127.5, 125.9 (2C), 113.0 (2C), 109.5 (2C), 107.8 (2C), 101.6, 69.1, 67.4, 56.5 (2C), 51.8, 46.5, 46.4, 44.6, 43.6, 41.5, 41.4, 40.3, 37.0; HRMS (ESI) 803.2539 for $[\text{M} + \text{Na}]^+$ (calcd 803.2534 for $\text{C}_{41}\text{H}_{40}\text{N}_4\text{NaO}_{12}$).

5.1.3.15. *N-[1-Oxyl-(4'-demethylepipodophyllotoxin)]-D-phenylalanine-4-(4-p-nitrophenyl-piperazine) carbamate (25)*. Yield: 69%; yellow powder solid; mp: 166–167 °C; $[\alpha]_{\text{D}}^{23} -53^\circ$ (c 0.1, CHCl_3); IR (KBr cm^{-1}) 3432, 2916, 1776, 1713, 1643, 1596, 1506, 1484, 1454, 1325, 1230, 1114, 1033, 996; ^1H NMR (600 MHz, CDCl_3) δ 8.13 (d, $J = 9.0$ Hz, 2H), 7.31 (t, $J = 7.2$ Hz, 2H), 7.23 (q, $J = 9.0$ Hz, 3H), 6.89 (s, 1H), 6.75 (d, $J = 9.6$ Hz, 2H), 6.55 (s, 1H), 6.31 (s, 2H), 6.04 (d, $J = 6.0$ Hz, 1H), 5.92 (d, $J = 7.2$ Hz, 1H), 5.76 (d, $J = 5.4$ Hz, 1H), 5.40 (s, 1H), 4.83 (t, $J = 9.6$ Hz, 1H), 4.67 (d, $J = 6.0$ Hz, 1H), 4.33 (t, $J = 7.2$ Hz, 1H), 3.90 (t, $J = 7.8$ Hz, 1H), 3.76 (s, 8H), 3.70 (d, $J = 6.0$ Hz, 1H), 3.54 (s, 1H), 3.19 (s, 2H), 3.03 (s, 2H), 2.92 (s, 1H), 2.90 (s, 1H), 2.73 (t, $J = 6.0$ Hz, 1H); ^{13}C NMR (150 MHz, CDCl_3) δ 174.3, 169.7, 155.0, 154.1, 148.5, 147.3, 146.5, 146.4, 139.2, 135.7, 130.5, 130.0, 129.5 (2C), 128.7 (2C), 127.7, 127.5, 125.9 (2C), 112.9, 110.4, 110.1, 109.6, 109.0, 107.9, 107.8, 101.6, 101.5, 69.1, 67.6, 56.4 (2C), 51.6, 46.5, 44.6, 43.7, 41.4, 40.3, 38.2, 37.0; HRMS (ESI) 803.2539 for $[\text{M} + \text{Na}]^+$ (calcd 803.2535 for $\text{C}_{41}\text{H}_{40}\text{N}_4\text{NaO}_{12}$).

5.1.3.16. *4'-Demethylepipodophyllotoxin 4 β , 4'-bis-(N-morpholino) carbamate (26)*. Yield: 69%; white powder solid; m.p.: 281–283 °C; $[\alpha]_{\text{D}}^{23} -36^\circ$ (c 0.3, CHCl_3); IR (KBr cm^{-1}) 3438, 2920, 1778, 1727, 1696, 1601, 1507, 1484, 1458, 1424, 1239, 1129, 1042, 997; ^1H NMR

(400 MHz, CDCl₃) δ 6.94 (s, 1H), 6.55 (s, 1H), 6.31 (s, 2H), 6.06 (d, $J = 3.6$ Hz, 1H), 6.00 (t, $J = 5.2$ Hz, 2H), 4.68 (d, $J = 5.4$ Hz, 1H), 4.39 (t, $J = 14.8$ Hz, 1H), 3.95 (t, $J = 8.8$ Hz, 1H), 3.92–3.72 (m, 5H), 3.71 (s, 9H), 3.62 (s, 2H), 3.53 (d, $J = 8.4$ Hz, 4H), 3.42 (s, 2H), 3.16 (dd, $J = 14.0, 4.8$ Hz, 1H), 3.00–2.92 (m, 1H); ¹³C NMR (100 MHz, CDCl₃) δ 174.3, 154.9, 153.5, 152.2 (2C), 149.0, 147.6, 137.0, 132.7, 128.7, 128.3, 110.4, 109.8, 107.8 (2C), 101.8, 69.5, 67.8, 66.8 (4C), 56.4 (2C), 44.5 (2C), 44.1 (2C), 41.9 (2C), 37.2; HRMS (ESI) 627.2189 for [M + H]⁺ (calcd 627.2185 for C₃₁H₃₅N₂O₁₂).

5.1.3.17. 4'-Demethylepipodophyllotoxin 4 β ,4'-bis-{N-[1-(4-nitrophenyl)piperazinyl]} carbamate (27). Yield: 73%; yellow powder solid; m.p.: 210–213 °C; [α]_D²³ –42° (c 0.3, CHCl₃); IR (KBr cm⁻¹) 3436, 2908, 1778, 1723, 1700, 1597, 1505, 1486, 1423, 1326, 1234, 1115, 1038, 997; ¹H NMR (400 MHz, CDCl₃) δ 8.17–8.13 (m, 4H), 6.94 (s, 1H), 6.87–6.81 (m, 4H), 6.55 (s, 1H), 6.32 (s, 2H), 6.05 (d, $J = 3.6$ Hz, 1H), 6.00 (d, $J = 6.4$ Hz, 2H), 4.66 (d, $J = 4.8$ Hz, 1H), 4.39 (t, $J = 16.4$ Hz, 1H), 3.99 (t, $J = 8.8$ Hz, 1H), 3.88 (s, 2H), 3.71 (s, 10H), 3.62 (s, 2H), 3.52 (s, 6H), 3.40 (s, 2H), 3.17 (dd, $J = 14.4, 4.8$ Hz, 1H), 3.04–2.94 (m, 1H); ¹³C NMR (100 MHz, CDCl₃) δ 174.3, 154.7, 154.6, 153.4, 152.1 (2C), 149.1, 147.7, 139.0, 137.1, 132.6, 128.4, 128.1, 126.1 (4C), 115.6, 113.1 (2C), 110.4, 109.7, 107.7 (2C), 101.9, 69.7, 67.8, 56.4 (2C), 47.0 (4C), 44.0 (2C), 43.5 (2C), 41.8 (2C), 37.2; HRMS (ESI) 889.2646 for [M + Na]⁺ (calcd 889.2651 for C₄₃H₄₂N₆NaO₁₄).

5.2. Biological evaluation

5.2.1. Cytotoxicity assays

Cells were incubated at 37 °C in a 5% CO₂ atmosphere. The MTT and Cell Counting Kit-8 (CCK-8) colorimetric assay were used to determined growth inhibition. The synthetic compounds **11–27** and reference compound VP-16 were dissolved in saline for five concentrations (0.001–100 μ M). For the HL-60, cells were plated in 96-well plates and exposed in quadplex well for 48 h. Then the CCK-8 was added to each well. After 4 h of incubation, the absorbance at λ_{450} was determined with a plate reader. For the A-549, HCT-8 and HeLa, cells were plated in 96-well plates and allowed to attach for 4–6 h, then exposed in quadplex well for 48 h. The media was aspirated, and 10 μ L of 5 mg/mL MTT solution (dilute in sterile PBS) diluted in serum-free media was added to each well. After 4 h of incubation, the solution was centrifuged for 10 min under 2000 rpm. The supernatant was mixed with 150 μ L DMSO, and shaken on an oscillator. The absorbance at λ_{570} was determined on a plate reader. IC₅₀ values were determined from a log plot of percent of control versus concentration.

5.2.2. Analysis of cell cycle by flow cytometry

For cell cycle analysis, we used the cervical carcinoma HeLa cell line grown in RPMI-1640 supplemented with 10% (v/v) heat-inactivated fetal calf serum, 2 mM L-glutamine, 100 units/mL penicillin, and 24 μ g/mL gentamicin and incubated at 37 °C in a humidified atmosphere of 5% CO₂ and 95% air. Untreated and drug-treated cells ((3–5) $\times 10^5$) were harvested and fixed overnight in 70% ethanol at 4 °C. Cells were then washed three times with PBS, incubated for 1 h with 1 mg/mL RNase A and 20 μ g/mL propidium iodide at room temperature, and analyzed with a flow cytometer (COULTER EPICS XL, USA) as described previously [21].

5.2.3. Western blot analysis

HeLa Cells (1 $\times 10^6$ cells) exposed to compound **19** were collected into tubes and then washed with PBS. Cell pellets were lysed with lyses buffer (50 mM Tris–HCl, pH 7.5, 10 mM EDTA, 0.2 M NaCl, 1.5 mM PMSF and 1% SDS). Cell lysates were boiled for 10 min, centrifuged and stored at –20 °C. Cell lysates containing 10–20 μ g protein were separated and transferred to nitrocellulose

filters. The blots were incubated with the corresponding antibodies and developed [32].

5.2.4. Circular dichroism studies

CT DNA was dissolved and annealed in 10 mM PBS (pH 7.2). To CT DNA in PBS (5 ml 50 μ g/mL) was added compound **19** in PBS (0, 0.5, 1.0, 2.0, 4.0 ml, 100 μ g/mL, respectively), and diluted to 10 ml. Same concentration sample of **19** in PBS was also prepared. The above mixture was incubated for 24 h in the dark at 37 °C. CD spectra were recorded on a JASCO J-810 spectrometer at 20 °C in quartz cells of 1 cm path length at increasing compound **19**/DNA ratio. Each sample solution was scanned in the range of 200–300 nm. The appropriate concentration samples of compound **19** in PBS were also determined as blank.

5.2.5. Fluorescence titrations

The binding of the compound **19** to CT DNA is performed by monitoring the changes in the emission spectral pattern of compound **19** in pH 7.2 BPS in the presence of increasing concentrations of CT DNA. After addition of indicated amount of DNA (0, 1, 2, 3, 4, 5, 6 μ M) to the compound **19** (0.5 μ M), the resulting solution was allowed to equilibrate for 5 min at 25 °C, excited at 383 nm followed by recording the emission spectral changes in the range of 765–790 nm. The appropriate concentration samples of CT DNA in PBS were also determined as blank.

Acknowledgments

Financial support from National Natural Science Foundation of China (No. 21372110, 81372177), and Natural Science Foundation of Gansu Province (No. 1208RJZA247) are gratefully acknowledged.

Appendix A. Supplementary data

Supplementary data related to this article can be found at <http://dx.doi.org/10.1016/j.ejmech.2013.09.053>.

References

- [1] S. Fulda, L. Galluzzi, G. Kroemer, Nat. Rev. Drug Discovery 9 (2010) 447–464.
- [2] S. Fulda, K.M. Debatin, Oncogene 25 (2006) 4798–4811.
- [3] U. Fischer, K. Schulze-Osthoff, Pharmacol. Rev. 57 (2005) 187–215.
- [4] C. Canela, R.M. Moraes, F.E. Dayana, D. Ferreira, Phytochemistry 54 (2000) 115–120.
- [5] M. Gordaliza, P.A. García, J.M.M. del Corral, M.A. Castro, M.A. Gómez-Zurita, Toxicol. 44 (2004) 441–459.
- [6] A. Jordan, J.A. Hadfield, N.J. Lawrence, A.T. McGown, Med. Res. Rev. 18 (1998) 259–296.
- [7] D.R. Budman, Semin. Oncol. 23 (1996) 8–14.
- [8] T.-S. Huang, C.-C. Lee, Y. Chao, C.-H. Shu, L.-T. Chen, L.-L. Chen, M.-H. Chen, C.-C. Yuan, W.-H. Peng, J. Pharm. Res. 16 (1999) 997–1002.
- [9] Y. Chen, T.-Y. Lin, J.-C. Chen, H.-Z. Yang, S.-H. Tseng, Anticancer Res. 26 (2006) 2149–2156.
- [10] J.M. Barret, C. Etievant, C. Baudouin, K. Skov, M. Charveron, B.T. Hill, Anticancer Res. 22 (2002) 187–192.
- [11] A. Kruczynski, I. Vandenbergh, A. Pillon, S. Pesnel, L. Goetsch, J.M. Barret, Y. Guminski, A. Le Pape, T. Imbert, C. Bailly, N. Guilbaud, Invest. New Drugs 29 (2011) 9–21.
- [12] F.A. Greco, J.D. Hainsworth, Semin. Oncol. 23 (1996) 40–47.
- [13] H. Xu, M. Lv, X. Tian, Curr. Med. Chem. 16 (2009) 327–349.
- [14] M. Duca, P. Meresse, E. Bertounesque, J. Med. Chem. 48 (2005) 593–603.
- [15] J.Y. Chang, F.S. Han, S.Y. Liu, Z.Q. Wang, K.H. Lee, Y.C. Cheng, Cancer Res. 51 (1991) 1755–1759.
- [16] A. Kamal, B.A. Kumar, P. Suresh, A. Juvekar, S. Zingde, Bioorg. Med. Chem. 19 (2011) 2975–2979.
- [17] S.-W. Chen, R. Xiang, J. Liu, X. Tian, Bioorg. Med. Chem. 17 (2009) 3111–3117.
- [18] Z.-W. Zhang, J.-Q. Zhang, L. Hui, S.-W. Chen, X. Tian, Eur. J. Med. Chem. 45 (2010) 1673–1677.
- [19] Y. Jin, J. Liu, W.-T. Huang, S.-W. Chen, L. Hui, Eur. J. Med. Chem. 413 (2011) 4056–4061.
- [20] S.-W. Chen, Y.-Y. Gao, N.-N. Gao, J. Liu, W.-T. Huang, L. Hui, Y. Jin, Y.-X. Jin, Bioorg. Med. Chem. Lett. 21 (2011) 7355–7358.

- [21] W.-T. Huang, J. Liu, J.-F. Liu, L. Hui, Y.-L. Ding, S.-W. Chen, *Eur. J. Med. Chem.* 49 (2012) 48–54.
- [22] J.-F. Liu, C.-Y. Sang, X.-H. Xu, L.-L. Zhang, X. Yang, L. Hui, J.-B. Zhang, S.-W. Chen, *Eur. J. Med. Chem.* 64 (2013) 621–628.
- [23] X. Liu, L.-L. Zhang, X.-H. Xu, L. Hui, J.-B. Zhang, S.-W. Chen, *Bioorg. Med. Chem. Lett.* 23 (2013) 3780–3784.
- [24] D. Chaturvedi, *Tetrahedron* 68 (2012) 15–45.
- [25] S. Ray, D. Chaturvedi, *Drugs Future* 29 (2004) 343–352.
- [26] S.M. Rahmanthullian, R.R. Tidwell, S.K. Jones, J.E. Hall, D.W. Boykin, *Eur. J. Med. Chem.* 43 (2008) 174–177.
- [27] S.J. Cho, A. Tropsha, M. Suffness, Y.C. Cheng, K.H. Lee, *J. Med. Chem.* 39 (1996) 1383–1395.
- [28] Y. You, *Curr. Pharm. Des.* 11 (2005) 1695–1717.
- [29] M.O. Hengartner, *Nature* 407 (2000) 770–776.
- [30] D. Hanahan, R.A. Weinberg, *Cell* 100 (2000) 57–70.
- [31] M.M. Pore, T.J.N. Hiltermann, F.A.E. Kruyt, *Cancer Lett.* 332 (2013) 359–368.
- [32] S.Y. Shin, Y.Y. Bahk, J. Ko, I.Y. Chung, Y.S. Lee, J. Downward, H. Eibel, P.M. Sharma, J.M. Olefsky, Y.H. Kim, B. Lee, Y.H. Lee, *EMBO J.* 25 (2006) 1093–1103.
- [33] R.M. Kluck, E. Bossy-Wetzels, D.R. Green, *Science* 275 (1997) 1132–1136.
- [34] C.M. Knudson, S.J. Korsmeyer, *Nat. Genet.* 16 (1997) 358–363.
- [35] Z. Xiao, S. Han, K.F. Bastow, K.H. Lee, *Bioorg. Med. Chem. Lett.* 14 (2004) 1581–1584.
- [36] S. Nahadevan, M. Palaiandavar, *Inorg. Chem.* 37 (1998) 3927–3934.
- [37] K. Tanaka, Y. Okahata, *J. Am. Chem. Soc.* 118 (1996) 10679–10683.
- [38] Z. Zhang, W. Huang, J. Tang, E. Wang, S. Dong, *Biophys. Chem.* 97 (2002) 7–16.
- [39] N. Kumari, B.K. Maurya, *Med. Chem. Commun.* 2 (2011) 1208–1216.